Temporal Decorrelation of X-Band Backscatter From Wind-Influenced Vegetation

RAM M. NARAYANAN, Member, IEEE
DAVID W. DOERR, Member, IEEE
DONALD C. RUNDQUIST
University of Nebraska

The temporal decorrelation characteristics of X-band Radar backscatter from wind-influenced vegetation were investigated using a short-range CW radar. Radar reflectance data were gathered on various types of individual trees from a distance of approximately 30 m. The windspeed was monitored during each measurement, which lasted 5 s. The crown cover and the mean leaf area of the trees were also recorded. Autocovariance plots were generated for each measurement, from which the decorrelation time was estimated. As expected, the return signals decorrelated faster at higher wind speeds. However, the decorrelation time was also found to depend on the tree type, tree structure, and leaf cover characteristics. Measured decorrelation times for moderate winds (7–9 m/s) were often between 40–60 ms, although the lowest decorrelation time measured under these conditions was 14 ms for the Eastern Cottonwood. In lighter winds (1–4 m/s), decorrelation times were much longer, and there was substantial spread in the data.

Manuscript received August 6, 1990; revised January 30, 1991.

IEEE Log No. 9104943.

The equipment used in this study was funded through NSF Research Equipment Grant ECS-8906018.

Authors' current addresses: R. M. Narayanan, Dept. of Electrical Engineering/Center for Electro-Optics, University of Nebraska, 209 N. Walter Scott Engineering Center, Lincoln, NE 68588; D. W. Doerr, J. A. Woollam Co., Lincoln, NE 68508; D. C. Rundquist, Center for Advanced Land Management Information Technologies, University of Nebraska, Lincoln, NE 68588.

I. INTRODUCTION

Large amounts of data have been gathered on the scattering of electromagnetic signals by various types of vegetated surfaces. The data are of interest to radar and communication systems engineers since the scattered signals, or clutter, can cause undesired interference. Remote sensing specialists also use such data to analyze terrestrial geophysical features. The scattering properties of natural targets are characterized by the normalized radar cross section, also called the radar backscatter coefficient, σ^0. Various databases which allow access to catalogued published data collected during the last few decades, have been compiled to facilitate easy access and retrieval (see, for example, [1]). In addition, many theoretical models have been developed and applied toward the understanding of surface and volume scattering from various types of vegetation [2–6].

We summarize our detailed experimental and theoretical study of temporal correlation properties of the radar reflected signals from wind-influenced vegetation. Since natural surfaces can be viewed as a collection of many elementary targets, the radar signals scattered from such distributed targets fluctuate randomly as their orientation changes, due to either target or radar motion [7]. Thus, the received power from vegetative targets follows a probability distribution which is subject to temporal decorrelation, caused by the movement of leaves and branches due to wind action. An understanding of this phenomenon, which is potentially useful in target identification and/or terrain classification, provides an analyst with additional pertinent information about the observed scene.

Decorrelation studies of vegetation moving in the wind thus far have been very general in nature [8–13], except for one fairly extensive investigation of this phenomenon [14]. In all of the above studies, however, no attempt was made to characterize radar returns from individual trees, or ensure concurrency of radar and windspeed acquisition data.

We report on the temporal decorrelation characteristics of X-Band radar reflections from various individual tree types under different windspeed conditions. Both deciduous and coniferous trees were studied, and the selected tree types represented wide variability in structural and leaf cover characteristics. Windspeed measurements were also made concurrently. Section II summarizes the experimental observations, and includes an overview of the radar system used in the study, the physical characteristics of trees investigated, and temporal decorrelation plots as a function of windspeed. In Section III, we apply existing models to the measured data. Conclusions are presented in Section IV.

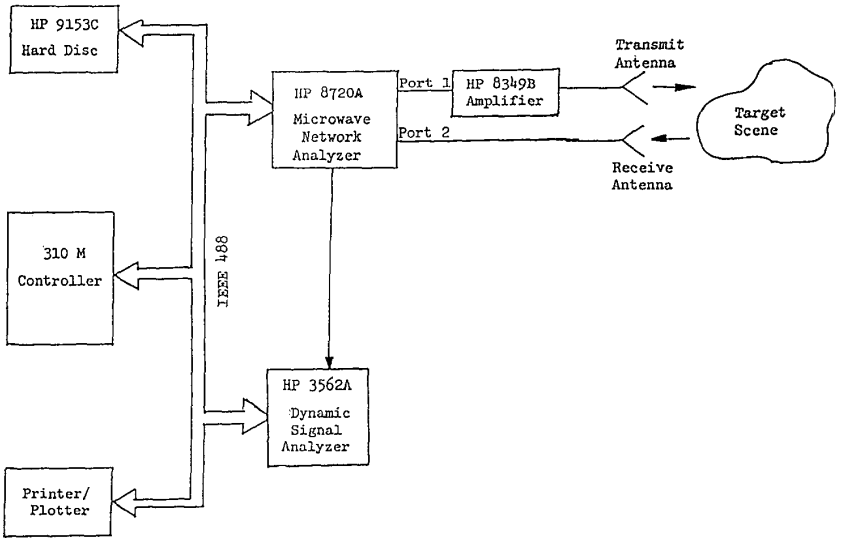

Fig. 1. Block diagram of radar system.

II. EXPERIMENTAL OBSERVATIONS

A. Radar System Overview

A block diagram of the short range CW radar system is shown in Fig. 1, and its specifications are summarized in Table I. The system consists of an HP 8720A network analyzer and an HP 8349B broadband amplifier. The HP 8720A is a compact self-contained unit with an integrated synthesized source, test set, and receiver, and is thus field deployable. The synthesized source operates from 130 MHz to 20 GHz with a frequency resolution of 100 kHz. The receiver dynamic range of 85 dB permits measurement of low-level cross-polarized signals. Transmit power amplification to +10 dBm is achieved through the use of the HP 8349B amplifier. Separate 24 in diameter broadband parabolic antennas are used, with beamwidths ranging from 3.5° at 8 GHz to 2.25° at 12.4 GHz. To improve isolation between the antennas, a metal plate is used as a shield.

The antennas are mounted atop a van, and the radar equipment and computers are housed within. Various other accessories such as the 310M controller, HP 9153C disc drive, HP 7475A plotter and HP 2225A printer are used for instrument control, data storage, and hardcopy outputs. Also available is an HP 3562A dual channel dynamic signal analyzer for baseband signal processing and analysis. This fast Fourier transform based (FFT-based) instrument, operating between 64 μHz and 100 KHz, enables us to characterize the statistics of radar reflected signals.

Windspeed is monitored using a Met One 014A anemometer whose digital outputs are directly sampled by the computer, at exactly the same time as the radar measurements. This ensures meaningful comparisons of decorrelation data at different windspeeds. The windspeed sensor is mounted on a 5 m mast attached to the top of the van behind the antennas. Since the sensor is stationed above the antennas, the air flow to the sensor is not blocked by the antennas.

TABLE I
Technical Specifications of Radar System

Radar System Parameters	
Type	CW
Frequency	8 GHz
Output Power	10 mW
IF Bandwidth	3000 Hz
Dynamic Range	70 dB
Antennas	
24 in Parabolic Reflectors	
Beamwidth	3.5 Deg
Polarization	Linear VV
Positioning	
Azimuth and Elevation	

B. Characteristics of Trees Studied

A list of the deciduous and coniferous trees that were investigated is shown in Table II. These trees were located on the periphery of a pecan orchard at the University of Nebraska East Campus in Lincoln, and were generally isolated from other trees. Fig. 2 shows a map of the experiment test site indicating various tree locations. Data were gathered from a distance of approximately 30 m from each tree, thus illuminating a spot size of about 1.8 m on the tree crown. Only the crown area of the trees were viewed from the side. Since the area between the trees and the radar van was free of any protruberances, we

TABLE II
Characteristics of Trees Studied

Tree Code	Tree Name	Height (meters)	Trunk Diameter (meters)	Crown Diameter (meters)	Branches or Twigs	Leafstalks or Needles
01	Austrian Pine	06	0.33	06	Stout	Stiff
02	Scotch Pine	08	0.35	07	Stout	Stiff
03	Scotch Pine	08	0.23	07	Stout	Stiff
04	Eastern Cottonwood	16	0.48	09	Stout	Slender
05	Scotch Pine	10	0.53	12	Stout	Stiff
06	Scotch Pine	08	0.72	11	Stout	Stiff
07	Scotch Pine	09	0.55	11	Stout	Stiff
08	Apple	05	0.67	08	Stout	Stiff
09	Eastern Black Walnut	12	0.55	14	Stout	Stalkless
10	Siberian Elm	16	0.62	12	Slender	Stiff
11	Siberian Elms	13 Avg.	0.29 Avg.	15 Group	Slender	Stiff
12	White Mulberry	10	0.82	16	Slender	Stiff
13	White Mulberries	12 Avg.	0.56 Avg.	14 Group	Slender	Stiff
15	Oaks	15 Avg.	0.49 Avg.	18 Group	—	—
16	Eastern Cottonwood	09	0.50	08	Stout	Slender

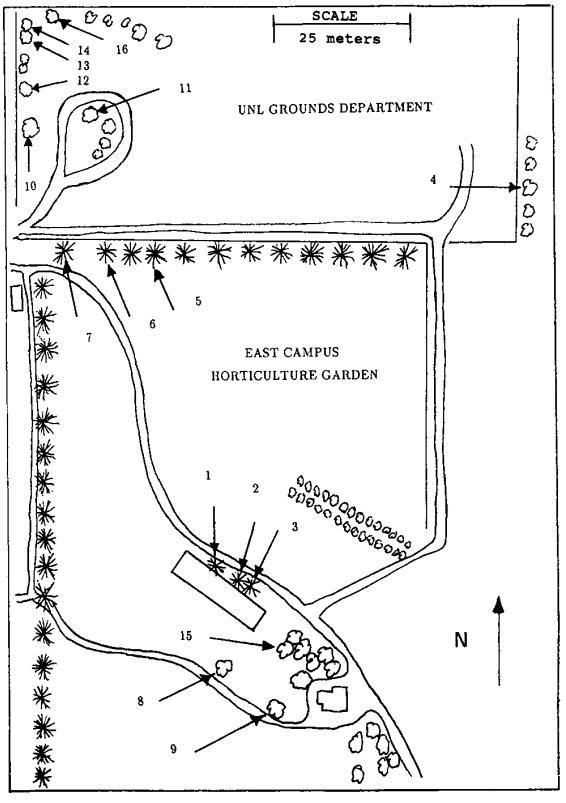

Fig. 2. Map of experiment test site.

anticipate the correlation distance of the wind to be higher than 30 m. In addition, the intent of this study was to relate the decorrelation phenomena to the general wind conditions in the neighborhood of the clutter cells.

The trees represented wide variability in structural and leaf-cover characteristics, and in their response to wind forces. In broadleaf trees, each individual leaf is flexible and attached to the twigs by a flexible leaf stalk, while coniferous trees have very thin, stiff needles [15]. The action of the wind on a vegetated structure is twofold. Even very light winds cause the leaves to flutter in a periodic fashion, which causes rapid fluctuations in the backscattered power. As the winds become stronger, in addition to the leaf flutter, larger structural units such as the trunk, branches and branchlets start to sway [16], causing slow variations in the backscattered power.

C. Decorrelation Time Related to Windspeed

Radar backscattered power was recorded for each individual tree over a 5 s duration. The polarization combination used was VV, i.e., vertical transmit/vertical receive. Data were gathered on different days over windspeeds ranging from 1 ms^{-1} to 12 ms^{-1}. The windspeed that was recorded was an average over a 1 min duration encompassing the radar reflectance measurement. For each

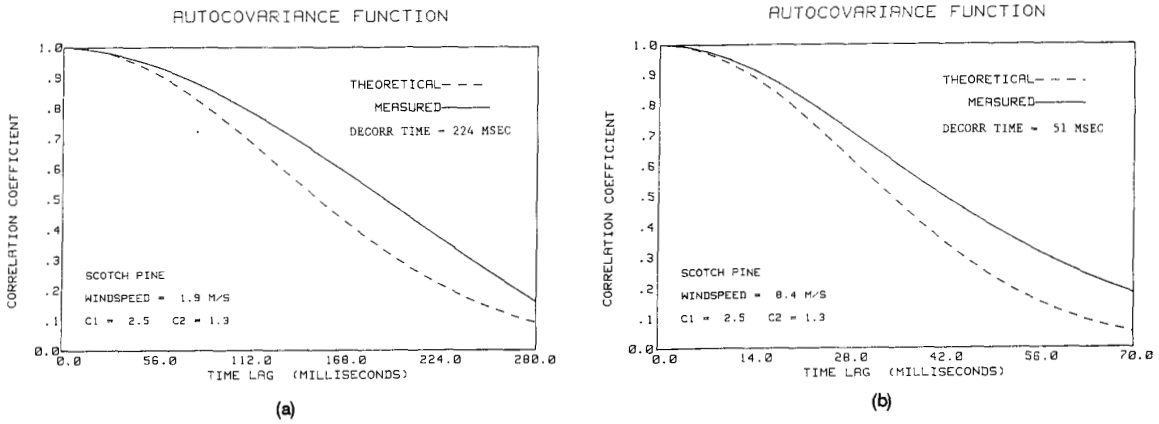

Fig. 3. Autocovariance function of Scotch pine tree at (a) low windspeeds, and (b) moderate windspeeds.

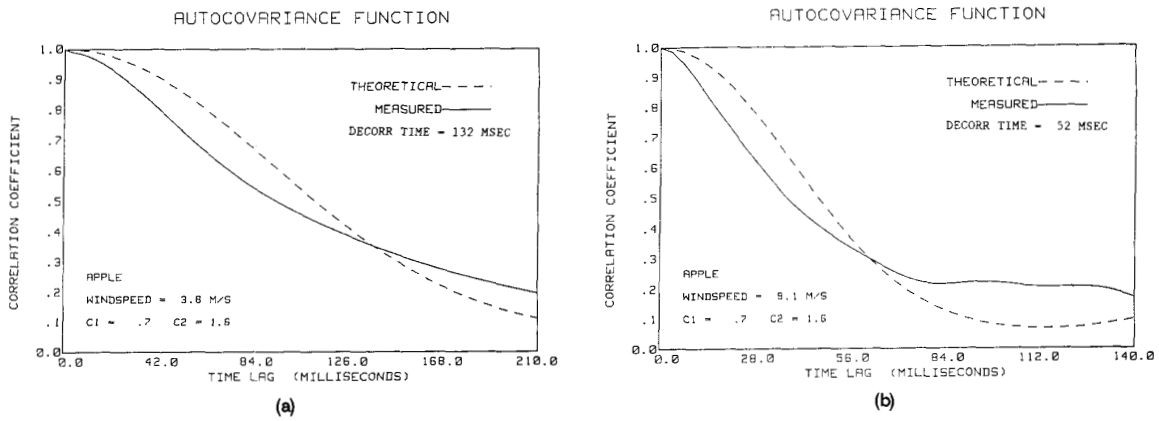

Fig. 4. Autocovariance function of apple tree at (a) low windspeeds, and (b) moderate windspeeds.

measurement, autocovariance plots were generated. Typical measured autocovariance plots for various trees at low and moderate windspeeds are shown in Figs. 3–8. Theoretical estimates obtained from the empirical formula derived in Section III are also shown for comparison. In general, it is seen that broadleaf (or deciduous) trees decorrelate more rapidly than needleleaf (or coniferous) trees, although in a few cases, the opposite situation occurs. Decorrelation time, defined as the time lag required for the autocovariance value to drop to 36.8% ($1/e$), is also indicated in the plots.

III. EMPIRICAL MODEL

A theoretical model for the autocovariance function of a rotating (or fluttering) ensemble of scatterers [9] is applied to the data. Since the radar system is stationary, we assume that the mean Doppler shift is zero. Referring to [9, eq. (33)] for the general case, the autocovariance function $R(\tau)$ is given by

$$R(\tau) = \exp[-\sigma_d^2\tau^2][\tfrac{2}{3} + \tfrac{1}{3}\exp[-2\sigma_r^2\tau^2]\cos 2\bar{\omega}_r\tau]^2 \tag{1}$$

where σ_d^2 is the Doppler frequency variance (due to linear oscillatory motion of the branches), $\bar{\omega}_r$ is the mean random flutter frequency, and σ_r^2 is the flutter frequency variance (which we assume to be zero henceforth to simplify the analysis). Furthermore, we assume that σ_d and $\bar{\omega}_r$ are independently proportional to the windspeed U. This assumption is intuitively obvious, since the branches and leaves vibrate and flutter more rapidly as windspeed increases.

Assuming $\sigma_d = C_1U$ and $\bar{\omega}_r = C_2U$, we obtain

$$R(\tau) = \exp[-C_1^2U^2\tau^2][\tfrac{2}{3} + \tfrac{1}{3}\cos 2C_2U\tau]^2 \tag{2}$$

where C_1 and C_2 are characteristic constants for each tree. Mean values of these constants, obtained by least-squares fit to the measured data for selected trees are given in Table III.

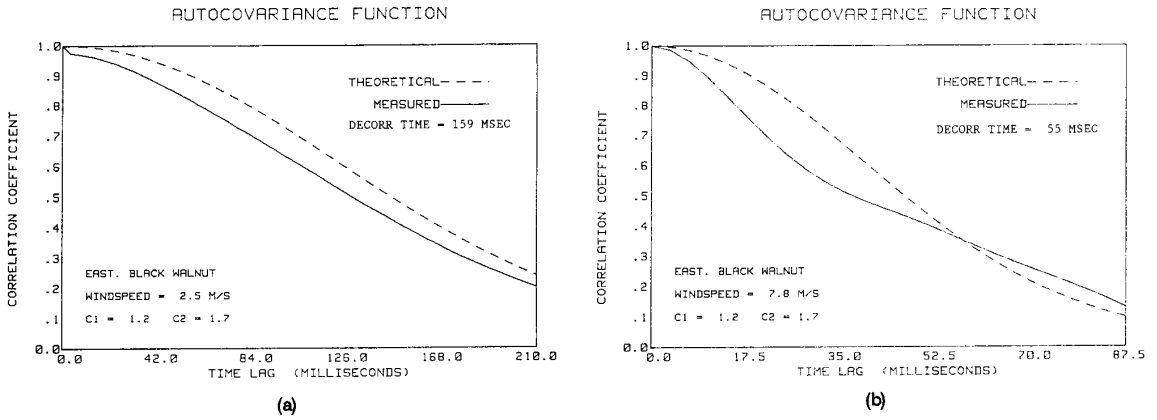

Fig. 5. Autocovariance function of eastern black walnut tree at (a) low windspeeds, and (b) moderate windspeeds.

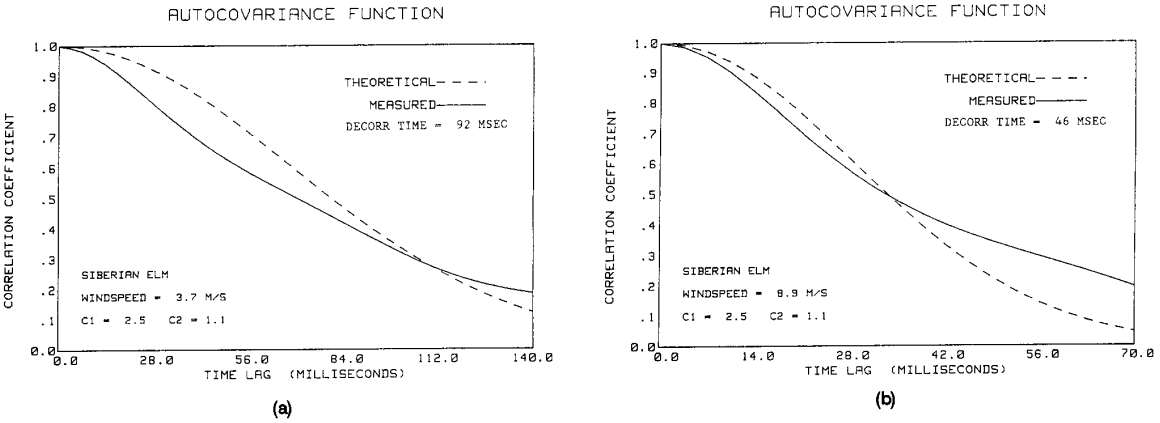

Fig. 6. Autocovariance function of Siberian elm tree at (a) low windspeeds, and (b) moderate windspeeds.

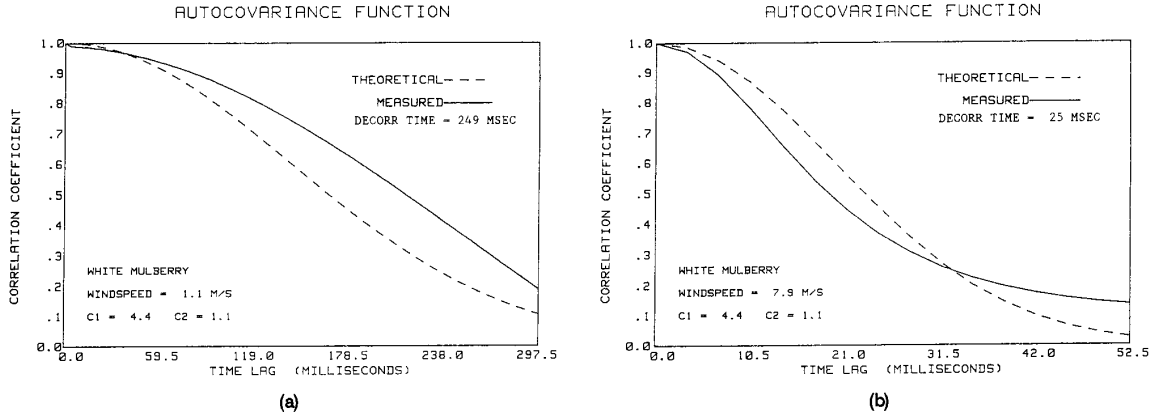

Fig. 7. Autocovariance function of white mulberry tree at (a) low windspeeds, and (b) moderate windspeeds.

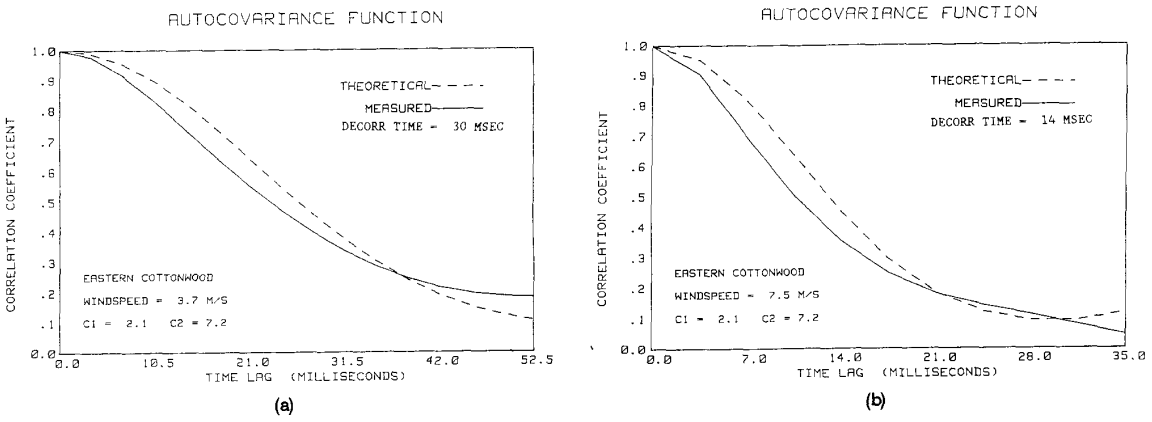

Fig. 8. Autocovariance function of eastern cottonwood tree at (a) low windspeeds, and (b) moderate windspeeds.

The theoretical autocovariance plots are also shown in Figs. 3–8. That the constants C_1 and C_2 are seen to have physical significance is borne out by the following. An apple tree subjected to a windspeed U of 5 m/s, has values of $\sigma_d = C_1 U = 3.5$ rad/s and $\bar{\omega}_r = C_2 U = 8$ rad/s. This translates to a vibration frequency of 0.55 Hz ($= \sigma_d/2\pi$) for the branch oscillation, and 1.27 Hz ($= \bar{\omega}_r/2\pi$) for the leaf flutter. Corresponding values for the white mulberry tree are 3.5 Hz and 0.88 Hz, respectively, while the cottonwood tree has corresponding values of 1.6 Hz and 5.7 Hz, respectively. The relatively high value for the branch oscillation frequency for the white mulberry tree is attributed to its slender twigs and branches, as compared with the stout branches for the other trees. Observe that the C_1 value of 4.4 for the white mulberry is higher than the C_1 values of other trees investigated. Similarly, the higher leaf flutter frequency of the cottonwood tree, attributed to its long slender leafstalks is apparent from its high C_2 value of 7.2, in contrast to lower values for the other trees.

Also of interest is the relationship between the decorrelation time, τ_d, and the windspeed U. Decorrelation time is defined by $R(\tau_d) = 1/e$. In theory, we can solve (2) at $\tau = \tau_d$, and obtain a relationship between τ_d and U. In order to simplify the analysis, we observe that the autocovariance function, $R(\tau)$ is related to the product $U\tau$. Thus, an intuitive inverse relationship between U and τ_d is evident. We therefore have

$$\tau_d = \frac{K}{U} \tag{3}$$

where K is again a characteristic constant for each tree.

The above simplified model is applied to the measured decorrelation time at different windspeeds, from which the value of K is estimated through least-squares fitting. These K values are also shown in Table III. Observe that the cottonwood tree has a much lower value for K, indicating that it decorrelates rapidly in wind.

TABLE III
Values of Decorrelation Constants C_1, C_2, and K for Each Tree

Tree Code	Tree Name	C_1 (rad/m)	C_2 (rad/m)	K (mm)
03	Scotch Pine	2.5	1.3	506
08	Apple	0.7	1.6	513
09	Eastern Black Walnut	1.2	1.7	447
10	Siberian Elm	2.5	1.1	416
13	White Mulberry	4.4	1.1	346
16	Eastern Cottonwood	2.1	7.2	78

Figs. 9–14 show measured decorrelation time as a function of windspeed for various trees. The theoretical curve, derived from (3) is also shown. We observe that the above inverse relationship matches fairly well the range of measured decorrelation times at moderate windspeeds (> 7.5 m/s). However, at low windspeeds, the large spread in measured decorrelation times essentially precludes any good fit between the model and the data. We hypothesize that this large variance in measured values around the empirical curve may be due to the fact that the effects of wind direction were ignored in this study. In addition, we conjecture that high windspeeds cause a more uniform motion of leaves and branches, which is fairly independent of wind direction and might explain the satisfactory fit to the inverse relationship. At low windspeeds, the tree is not in uniform motion; leaves facing the wind flutter more rapidly than leaves on the opposite side, and this explains the large spread in measured decorrelation times under these conditions.

IV. CONCLUSIONS

Our paper quantifies the effects of wind on the decorrelation time of X-Band radar backscatter

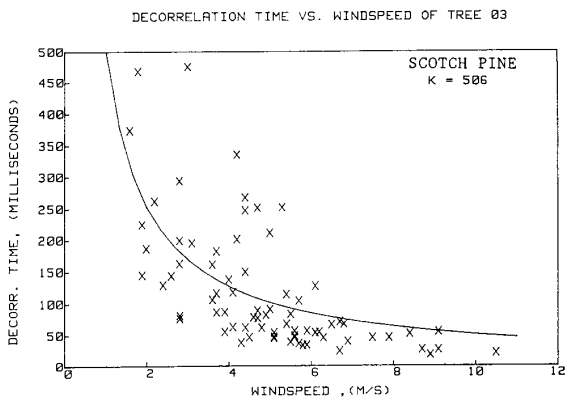

Fig. 9. Measured and computed decorrelation time versus windspeed for Scotch pine.

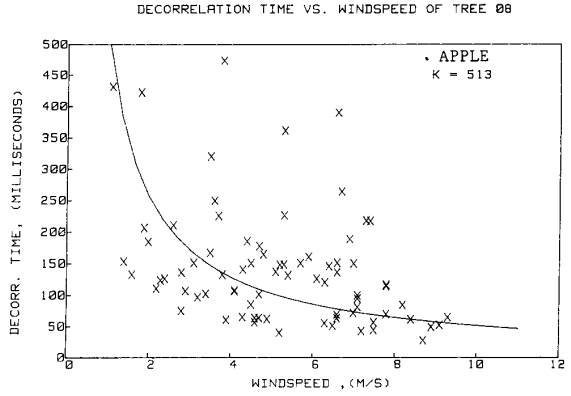

Fig. 10. Measured and computed decorrelation time versus windspeed for apple.

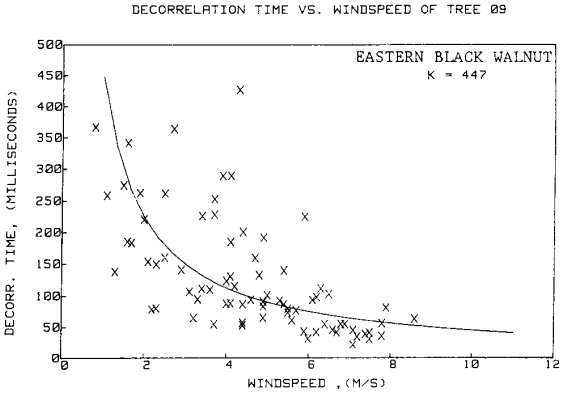

Fig. 11. Measured and computed decorrelation time versus windspeed for eastern black walnut.

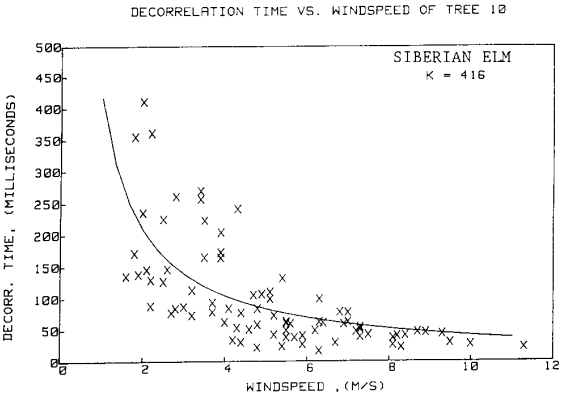

Fig. 12. Measured and computed decorrelation time versus windspeed for Siberian elm.

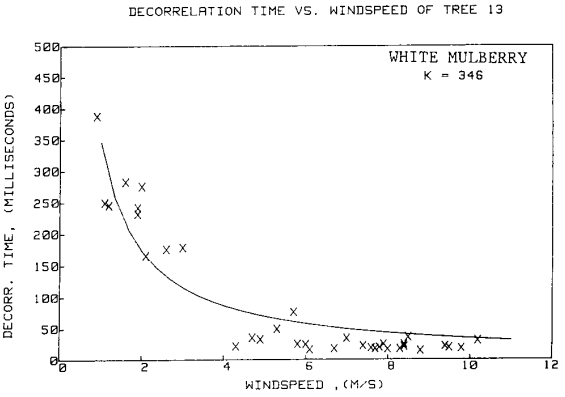

Fig. 13. Measured and computed decorrelation time versus windspeed for white mulberry.

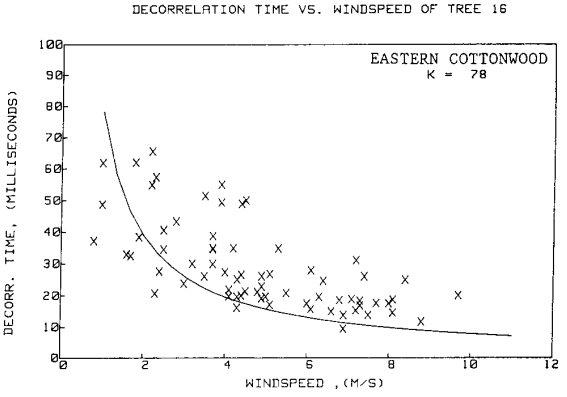

Fig. 14. Measured and computed decorrelation time versus windspeed for eastern cottonwood.

from individual trees. The measured autocovariance function closely resembles a simple theoretical model developed in [9]. We also find that different trees respond differently to wind, and that decorrelation times generally fall inversely at higher windspeeds. Measured data also indicate that the variance of the decorrelation time is very large at low windspeeds, and researchers and system designers need to be aware of this experimentally observed fact.

ACKNOWLEDGMENT

We appreciate the assistance of J. P. Dalton during the field measurements.

REFERENCES

[1] Borel, C. C., McIntosh, R. E., Narayanan, R. M., and Swift, C. T. (1986)
FINRACS—A computer program for research of the scattering of radar signals by natural surfaces.
IEEE Transactions Geoscience and Remote Sensing, **GE-24** (1986), 1020–1022.

[2] Deane, J. M. (1987)
Modelling radar backscatter from vegetation.
GEC Journal of Research, **5** (1987), 182–188.

[3] Attema, E. P. W., and Ulaby, F. T. (1978)
Vegetation modeled as a water cloud.
Radio Science, **13** (1978), 357–364.

[4] Borel, C. C., and McIntosh, R. E. (1986)
A backscattering model for various foliated deciduous tree types at millimeter wavelengths.
In *Proceedings of the IGARSS '86 Symposium*, Zurich, Sept. 1986, 867–872.

[5] Seker, S. S. (1986)
Microwave backscattering from a layer of randomly oriented discs with application to scattering from vegetation.
IEE Proceedings, Pt. H, **133** (1986), 497–502.

[6] Fung, A. K., Chen, M. F., and Lee, K. K. (1987)
Fresnel field interaction applied to scattering from a vegetation layer.
Remote Sensing of Environment, **23** (1987), 35–50.

[7] Moore, R. K. (1983)
Radar fundamentals and scatterometers.
In D. S. Simonett (Ed.), Chapter 9 in *Manual of Remote Sensing*, Vol. 1.
Falls Church, VA: American Society for Photogrammetry and Remote Sensing, 1983, 369–427.

[8] Rosenbaum, S., and Bowles, L. W. (1974)
Clutter return from vegetated areas.
IEEE Transactions on Antennas and Propagation, **AP-22** (1974), 227–236.

[9] Wong, J. L., Reed, I. S., and Kaprielian, Z. A. (1967)
A model for the radar echo from a random collection of rotating dipole scatterers.
IEEE Transactions on Aerospace and Electronic Systems, **AES-3** (1967), 171–178.

[10] Barlow, E. J. (1949)
Doppler radar.
Proceedings of the IRE, **37** (1949), 340–355.

[11] Ivey, H. D., Long, M. W., and Widerquist, V. R. (1956)
Polarization properties of echoes from vehicles and trees.
In *Record of the Second Annual Radar Symposium*, Ann Arbor, MI, 1956.

[12] Fishbein, W., Graveline, S. W., and Rittenbach, O. E. (1967)
Clutter attenuation analysis.
Technical report ECOM-2808, U.S. Army Electronics Command, Mar. 1967.

[13] Hayes, R. D. (1979)
95 GHz pulsed radar returns from trees.
In *IEEE EASCON-79 Conference Record*, **2** (1979), 353–356.

[14] Billingsley, J. B., and Larrabee, J. F. (1987)
Measured spectral extent of L- and X-Band radar reflections from wind-blown trees.
Project report CMT-57, M.I.T. Lincoln Laboratory, Lexington, MA, Feb. 6, 1987.

[15] Banks, C. C. (1970)
The strength of trees.
Journal of the Institute of Wood Science, **5** (1970), 44–50.

[16] Mayhead, G. J. (1973)
Sway periods of forest trees.
Scottish Forestry, **27** (1973), 19–23.

Ram Narayanan (S'83—M'88) received his B.Tech degree in electrical engineering from the Indian Institute of Technology, Madras, India, in 1976 and the Ph.D. degree in electrical and computer engineering from the University of Massachusetts, Amherst, in 1988.

From 1976 to 1983, he was employed as a Research and Development Engineer at Bharat Electronics Ltd., Ghaziabad, India, where he was involved in the development of microwave troposcatter communication equipment. He joined the Microwave Remote Sensing Laboratory at the University of Massachusetts, Amherst, in 1983 as a Research Assistant where he worked in the areas of electromagnetic scattering and propagation at millimeter wavelengths, and developed a unique high power 215 GHz radar as part of his doctoral research. He joined the faculty of Electrical Engineering at the University of Nebraska, Lincoln, in 1988, and shortly thereafter established a microwave and optical remote sensing capability. He has also been associated with the Center for Electro-Optics since 1989. His current research interests are in the areas of terrain scattering at microwave to optical frequencies, and the development of remote sensing systems for environmental, agricultural, and meteorological applications.

Dr. Narayanan is a member of Institute of Electrical and Electronics Engineers, American Geophysical Union, ASPRS, International Scientific Radio Union Commission F, International Electromagnetics Academy, a Graduate Faculty Fellow of the University of Nebraska, and a Fellow of the Center for Great Plains Studies.

David W. Doerr (S'84—M'86) received the B.S.E.E. and M.S.E.E. degrees from the University of Nebraska, Lincoln in 1986 and 1990, respectively.

In 1986, he joined the Radar Laboratory at McDonnell Douglas Aircraft Company, St. Louis, MO, where he supported flight testing and software development of the radar system in the F-15 aircraft. In 1990, he joined the J. A. Woollam Company, Lincoln, NE, where he has worked on extending the spectral range and speed of ellipsometers used for thin film characterization.

Donald C. Rundquist is Professor and Research Scientist with the Conservation and Survey Division, Institute of Agriculture and Natural Resources, University of Nebraska, Lincoln. He also serves as Director of the Division's Center for Advanced Land Management Information Technologies (CALMIT), teaches courses in remote sensing and digital image processing, and holds adjunct appointments in the Departments of Agricultural Meteorology, Geography, and Geology. One of his primary areas of interest, beginning in the early 1970s, has been the application of remote sensing to natural-resources issues. His current research interests include high spectral resolution remote sensing of the community structure and stress responses of ponds, lakes, and reservoirs, coarse-resolution satellite-based analyses of terrestrial vegetation dynamics, and farm-level geographic information systems.